

Spin Hall effect emerging from a noncollinear magnetic lattice without spin-orbit coupling

Yang Zhang,^{1,2} Jakub Železný,¹ Yan Sun,¹ Jeroen van den Brink,^{2,3} and Binghai Yan^{4,*}

¹*Max Planck Institute for Chemical Physics of Solids, 01187 Dresden, Germany*

²*Leibniz Institute for Solid State and Materials Research,*

IFW Dresden, 01069 Dresden, Germany

³*Institute for Theoretical Physics, TU Dresden, 01069 Dresden, Germany*

⁴*Department of Condensed Matter Physics,*

Weizmann Institute of Science, 7610001 Rehovot, Israel

Abstract

The spin Hall effect (SHE), which converts a charge current into a transverse spin current, has long been believed to be a phenomenon induced by the spin-orbit coupling. Here, we identify an alternative mechanism to realize the intrinsic SHE through a noncollinear magnetic structure that breaks the spin rotation symmetry. No spin-orbit coupling is needed even when the scalar spin chirality vanishes, different from the case of the topological Hall effect and topological SHE reported previously. In known noncollinear antiferromagnetic compounds Mn_3X ($X = \text{Ga}, \text{Ge}, \text{and Sn}$), for example, we indeed obtain large spin Hall conductivities based on *ab initio* calculations.

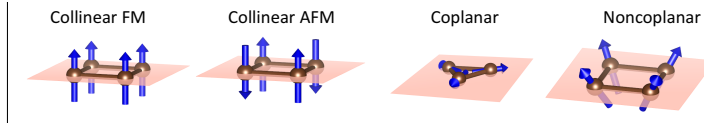
I. INTRODUCTION

The spin Hall effect (SHE)¹ is one of the most important ways to create and detect spin currents in the field of spintronics, which aims to realize low-power-consumption and high-speed devices.² It converts electric currents into transverse spin currents and vice versa. The SHE in materials is generally believed to rely on spin-orbit coupling (SOC)^{1,3-5}. In typical SHE devices, the generated spin current is injected into a ferromagnet (FM) and consequently switches its magnetization via the spin-transfer torque^{6,7} or drives an efficient motion of magnetic domain walls.^{8,9}

The SHE is conceptually similar to the well established anomalous Hall effect (AHE). In recent decades, the understanding of the intrinsic AHE¹⁰ and intrinsic SHE^{11,12} was significantly advanced based on the concept of the Berry phase,¹³ which originates directly from the electronic band structure. Although the AHE requires the existence of SOC in a FM, it also appears in a non-coplanar magnetic lattice without SOC, where an electron acquires a Berry phase by hopping through sites with a noncoplanar magnetic structure (nonzero scalar spin chirality)^{14,15}, later referred as the topological Hall effect (THE)¹⁶. Thus, in experiment the THE-induced Hall signal is considered as a signature of the skyrmion phase with chiral spin texture^{17,18}. Provoked by the THE, recent numerical simulations of the spin scattering by a single skyrmion indicated the presence of a finite SHE even without SOC¹⁹⁻²¹, which is termed as a topological SHE. Thus, the topological SHE has been presumed to stem from the Berry phase due to the nonzero spin chirality of the skyrmion. However, the origin of the spin current is illusive in the topological SHE, for it is hard to separate it from the spin-polarized charge current of the THE. Here, we pose new questions one step further. Is the skyrmion-like spin texture (nonzero scalar spin chirality) always necessary to generate a SHE without SOC? What is the generic condition for a SHE without SOC?

In this article, we propose a mechanism to realize the SHE with the noncollinear magnetic structure but without SOC. The crucial role of SOC is to break the spin rotational symmetry (SRS) in SHE. Alternatively, it is known that common noncollinear magnetic textures can also violate the SRS, thus resulting in the SHE. Different from the THE and topological SHE in symmetry, such an SHE appears universally for the noncollinear magnetic lattice, regardless of the scalar spin chirality. For example, it can even emerge in a coplanar magnetic

structure where the scalar spin chirality is zero. Here, we first prove the principle from the symmetry analysis in a simple lattice model. Then, we demonstrate the existence of a strong SHE in several known materials Mn_3X ($X = \text{Ga}, \text{Ge}, \text{and Sn}$)^{22,23} by *ab initio* calculations without including SOC.



		Collinear FM	Collinear AFM	Coplanar	Noncoplanar
Without SOC	AHE	×	×	×	✓
	SHE	×	×	✓	✓
With SOC	AHE	✓	×	✓	✓
	SHE	✓	✓	✓	✓

FIG. 1. Symmetry conditions for the existence (\checkmark) or absence (\times) of AHE and SHE in collinear FM, collinear AFM, coplanar, and noncoplanar magnetic lattices with and without SOC. Note that the SHE is symmetry allowed when the magnetic ordering is coplanar (but noncollinear) even without SOC (see text).

II. RESULTS

Double-exchange model and symmetry analysis – The existence of the SHE and AHE in metals is determined by symmetry (in insulators apart from symmetry also the topology of the electronic structure is important). The symmetry of magnetic systems is normally described in terms of magnetic space groups, which contain, apart from the spatial symmetry operations, also the time-reversal symmetry operation. In absence of SOC (or other terms in the Hamiltonian that couple the magnetic moments to the lattice such as the shape anisotropy), however, the symmetry of the magnetic systems is higher than that contained in the magnetic space groups since the spins can be rotated independently of the lattice.

This can be illustrated by considering the following minimal Hamiltonian

$$H = t \sum_{\langle ij \rangle \alpha} c_{i\alpha}^\dagger c_{j\alpha} - J \sum_{i\alpha\beta} (\boldsymbol{\sigma} \cdot \mathbf{n}_i)_{\alpha\beta} c_{i\alpha}^\dagger c_{i\beta}, \quad (1)$$

known as the double-exchange model (*s-d* model)^{24–26} which describes itinerant *s* electrons interacting with local *d* magnetic moments. We assume that magnetic moments are only contributed by the spin degrees of freedom. Here, α and β stand for spin up and spin down, respectively. The first term is the nearest neighbor hopping term with $\langle ij \rangle$ denoting the nearest neighbor lattice sites. In the second term, J is the Hund's coupling strength between the conduction electron and the on-site spin moment, $\boldsymbol{\sigma}$ is the vector of Pauli matrices, and \mathbf{n}_i is the spin magnetic moment on site i . The magnetic texture is defined by the pattern of \mathbf{n}_i . In such a Hamiltonian, spin rotation only rotates the magnetic moments \mathbf{n}_i . The corresponding symmetry groups are thus formed by combining the magnetic space groups with spin rotations.^{27,28} Such symmetry groups are referred to as spin-space groups. They apply generally for non-interacting Hamiltonians in absence of spin-orbit coupling.

We focus here only on the intrinsic contribution to the AHE and SHE, however, the other (extrinsic) contributions have the same symmetry and thus the symmetry discussion in the following is general. The intrinsic AHE and intrinsic SHE are well characterized via the Berry curvature formalism.^{1,5,10,13} The anomalous Hall conductivity (AHC) $\sigma_{\alpha\beta}$ can be evaluated by the integral of the Berry curvature $\Omega_{\alpha\beta}^n(\mathbf{k})$ over the Brillouin zone (BZ) for all the occupied bands, where n is the band index. It should be noted that this method can also be applied to the THE, although it is commonly interpreted using the real space spin texture. Here, $\sigma_{\alpha\beta}$ corresponds to a 3×3 matrix and indicates a transverse Hall current j_α generated by a longitudinal electric field \mathbf{E} , which satisfies $J_\alpha = \sigma_{\alpha\beta} E_\beta$. Within a linear response, Berry curvature can be expressed as

$$\Omega_{n,\alpha\beta}(\vec{k}) = 2i\hbar^2 \sum_{m \neq n} \frac{\langle \psi_{n\mathbf{k}} | \hat{v}_\alpha | \psi_{m\mathbf{k}} \rangle \langle \psi_{m\mathbf{k}} | \hat{v}_\beta | \psi_{n\mathbf{k}} \rangle}{(E_n(\vec{k}) - E_m(\vec{k}))^2}, \quad (2)$$

where n and m are band indices, and $\psi_{n\mathbf{k}}$ and $E_{n\mathbf{k}}$ denote the Bloch wave functions and eigenvalues, respectively, and \hat{v} is the velocity operator. Replacing the velocity operator with the spin current operator $\hat{J}_\alpha^\gamma = \frac{1}{2} \{ \hat{v}_\alpha, \hat{s}_\gamma \}$, where \hat{s}_γ is the spin operator, we obtain the

spin Berry curvature and corresponding spin Hall conductivity (SHC),

$$\begin{aligned}\sigma_{\alpha\beta}^{\gamma} &= \frac{e}{\hbar} \sum_n \int_{BZ} \frac{d^3\mathbf{k}}{(2\pi)^3} f_n(\mathbf{k}) \Omega_{n,\alpha\beta}^{\gamma}(\mathbf{k}), \\ \Omega_{n,\alpha\beta}^{\gamma}(\mathbf{k}) &= 2i\hbar^2 \sum_{m \neq n} \frac{\langle \psi_{n\mathbf{k}} | \hat{J}_{\alpha}^{\gamma} | \psi_{m\mathbf{k}} \rangle \langle \psi_{m\mathbf{k}} | \hat{v}_{\beta} | \psi_{n\mathbf{k}} \rangle}{(E_{n\mathbf{k}} - E_{m\mathbf{k}})^2}.\end{aligned}\tag{3}$$

The SHC ($\sigma_{\alpha\beta}^{\gamma}$; $\alpha, \beta, \gamma = x, y, z$) is a third-order tensor ($3 \times 3 \times 3$) and represents the spin current $J_{s,\alpha}^{\gamma}$ generated by an electric field \mathbf{E} via $J_{s,\alpha}^{\gamma} = \sigma_{\alpha\beta}^{\gamma} E_{\beta}$, where $J_{s,\alpha}^{\gamma}$ is a spin current flowing along the α -direction with the spin-polarization along the γ -direction, and $f_n(\mathbf{k})$ is the temperature dependent Fermi-Diract distribution.

We know that AHE vanishes while SHE remains if the time-reversal symmetry (operator T) exists in the system. In Eq. 2, T reverses the velocities $\hat{v}_{\alpha,\beta}$ and brings an additional “-” sign by the complex conjugate. Thus, $\sigma_{\alpha\beta} = 0$ owing to $\Omega_{n,\alpha\beta}(\vec{k}) = -\Omega_{n,\alpha\beta}(-\vec{k})$. In contrast, In Eq. 3, T generates one more “-” sign by reversing the spin in J_{α}^{γ} . Then, $\sigma_{\alpha\beta}^{\gamma}$ can be nonzero since $\Omega_{n,\alpha\beta}^{\gamma}(\vec{k})$ is even in k -space. In a magnetic system without SOC, T is broken, but a combination of T and a spin rotation (operator S) can still be a symmetry. For example, a coplanar magnetic system shows a TS symmetry, in which S rotates all spins by 180° around the axis perpendicular to the plane. Since S does not act on $\hat{v}_{\alpha,\beta}$, TS causes vanishing $\sigma_{\alpha\beta}$ just as T alone. In a general noncoplanar magnetic lattice, the TS symmetry is naturally broken, because one cannot find a common axis about which all spins can be rotated 180° at the same time, and thus the AHE can exist without SOC.

The situation is different for the SHE since J_{α}^{γ} in Eq. 3 contains an additional spin operator. As a consequence, (assuming that S is a rotation around the z axis) TS forces $\Omega_{n,\alpha\beta}^{x/y}(\vec{k})$ to be odd where spin \hat{s}_x or \hat{s}_y is reversed by TS , but $\Omega_{n,\alpha\beta}^z(\vec{k})$ to be even where \hat{s}_z is unchanged by TS . Then, one can obtain zero $\sigma_{\alpha\beta}^{x/y}$ but nonzero $\sigma_{\alpha\beta}^z$. In a collinear magnetic lattice there exists more than one spin rotation S such that TS is a symmetry of the system and thus all of the $\sigma_{\alpha\beta}^{\gamma}$ components have to vanish. Therefore, we can argue that SHE can exist without SOC in general noncollinear magnetic lattices, regardless of FM, AFM, or the scalar spin chirality (coplanar or noncoplanar). In contrast, the AHC is zero for a coplanar magnetic lattice (zero scalar spin chirality), since TS acts as T alone in Eq. 2.

When SOC is included, SHE is allowed by symmetry in any crystal,²⁹ while the AHE on the other hand can be present in magnetic systems that are not symmetric under time reversal combined with a translation or inversion (for example, a conventional collinear

AFM). We summarize the necessary conditions for the existence of AHE and SHE in systems with and without SOC in Fig. 1.

To demonstrate that the SHE can indeed be nonzero without SOC, we consider the s - d Hamiltonian (1) projected on a kagome lattice with the so-called $q = 0$ magnetic order, shown in Fig. 2(a). Such a coplanar AFM order is well studied in theory^{14,30} and appears in many realistic materials even at room temperature, for example Mn_3X ($X = \text{Ir}, \text{Ga}, \text{Ge}, \text{and Sn}$)^{22,23,31-34} as we discuss in the following. For comparison, the SOC effect is also considered by adding to H in Eq. 1,

$$H_{\text{so}} = it_2 \sum_{\langle ij \rangle \alpha \beta} v_{ij} (\boldsymbol{\sigma} \cdot \mathbf{n}_{ij})_{\alpha\beta} c_{i\alpha}^\dagger c_{j\beta}, \quad (4)$$

where v_{ij} is the antisymmetric Levi-Civita symbol and \mathbf{n}_{ij} are a set of coplanar vectors anticlockwise perpendicular to the lattice vector R_{ij} , as defined in Ref. 30 and t_2 is the SOC strength.

We first analyze the symmetry of the SHC tensor for the $q = 0$ magnetic order. Note that we use the Cartesian coordinate systems defined in Fig. 2. As discussed above, the existence of the TS symmetry leaves only $\sigma_{\alpha\beta}^z$ terms in the absence of SOC. Further, the combined symmetry TM_x , in which M_x is the mirror reflection along x and flips \hat{s}_z and \hat{v}_x in Eq. 3, leads to $\sigma_{xx}^z = \sigma_{yy}^z = 0$. We further obtain only two nonzero SHC tensor element $\sigma_{xy}^z = -\sigma_{yx}^z$ by considering the three-fold rotation around z . The magnetic order shown in Fig. 2(b) will also be relevant for the discussion in the following. This magnetic configuration differs from the $q = 0$ case only by a two-fold spin rotation around the y -axis and thus, without SOC its symmetry is exactly the same as that of the $q = 0$ case.

Setting the Hund coupling constant $J = 1.7t$ and SOC strength $t_2 = 0$, we calculate the spin Berry curvature via Eq. 3. As expected, we find nonzero SHC σ_{xy}^z fully in agreement with the symmetry considerations. Figures 3a and 3b show the band structures with $t_2 = 0$ and $t_2 = 0.2t$, respectively. One can see that SOC modifies slightly the band structure by gapping some band crossing points such as the BZ corners (K). Without SOC, we already observe nonzero σ_{xy}^z , while adding SOC reduces σ_{xy}^z slightly at the Fermi energy that is set between the first and second bands at about -2.7 eV. We plot corresponding spin Berry curvature Ω_{xy}^z in the hexagonal BZ in Figs. 3d and 3e. Large Ω_{xy}^z appears in the BZ without SOC, leading to net σ_{xy}^z . The SOC simply brings an extra contribution to σ_{xy}^z at the band anti-crossing region around the K point.

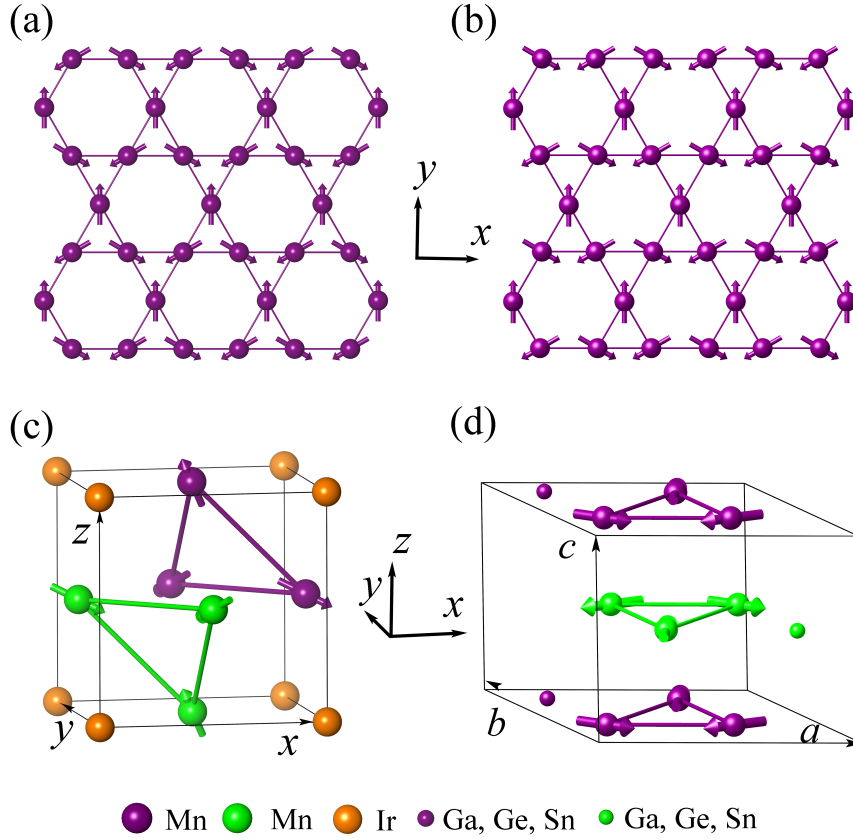


FIG. 2. Noncollinear order in kagome lattice and the magnetic structure of Mn_3Ir and Mn_3X ($\text{X} = \text{Ga}, \text{Ge}, \text{and Sn}$). (a) The $q = 0$ order in the kagome lattice, with magnetic moments located as 2D Mn plane in Mn_3Ir , (b) Two-fold spin rotation around y -axis of configuration (a), corresponding to Mn planes in Mn_3X ($\text{X} = \text{Ga}, \text{Ge}, \text{Sn}$), (c) The face-centered cubic crystal structure of Mn_3Ir , (d) The hexagonal crystal structure of Mn_3X ($\text{X} = \text{Ga}, \text{Ge}, \text{and Sn}$).

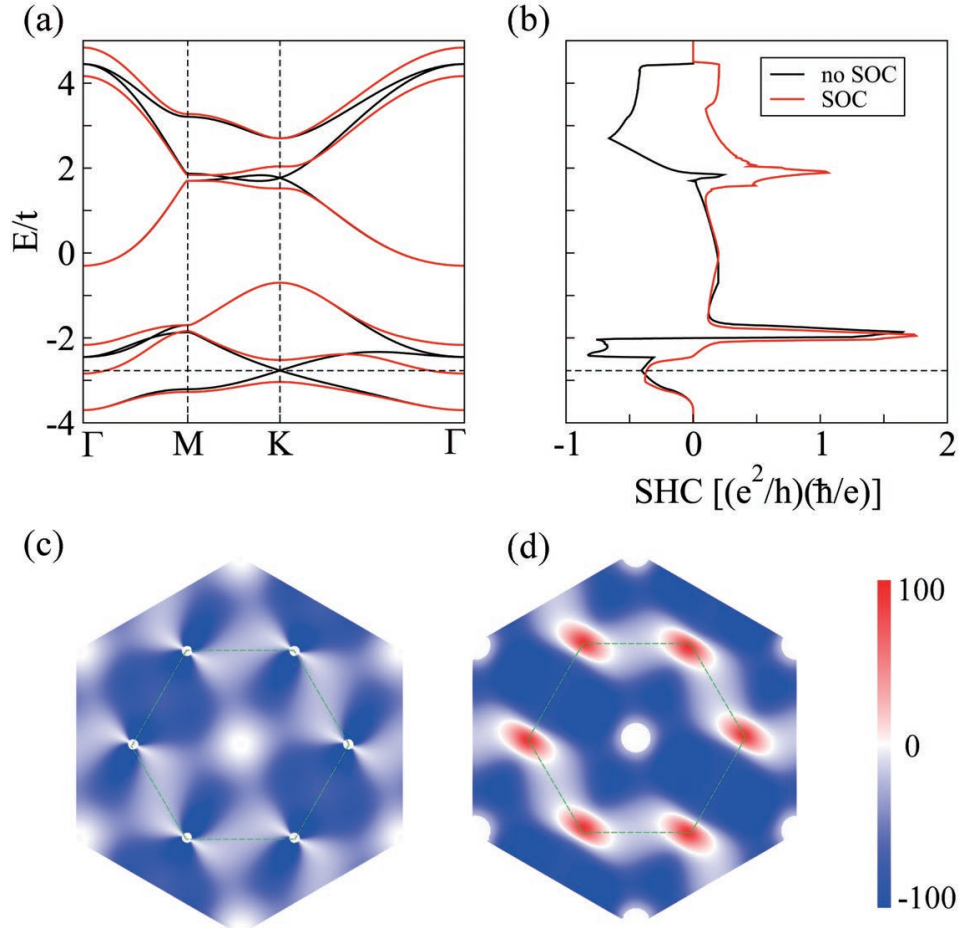


FIG. 3. Electronic band structures $q = 0$ order in kagome lattice, (a) without and with SOC. (b) Energy-dependent SHC σ_{xy}^z . (c) Spin Berry curvature Ω_{xy}^z distribution of first BZ at Fermi energy -2.7 eV (horizontal line) without SOC and (d) with SOC.

Realistic materials – After proving the principle, we now identify materials that show strong SHE with negligible contribution from SOC. We naturally consider Mn_3X ($\text{X}=\text{Ga}, \text{Ge}, \text{Sn}, \text{and Ir}$) compounds, since they exhibit non:collinear AFM order at room temperature (the AFM Néel temperature is over 365 K). Our recent *ab initio* calculations showed a sizable intrinsic SHE by including SOC³⁴. Here, we further point out that SHE still presents without SOC and SOC actually plays a negligible effect for SHE in these materials.

The primitive unit cell of Mn_3Ga , Mn_3Ge and Mn_3Sn (space group $P6_3/mmc$, No. 194) includes two Mn_3X planes that are stacked along the c -axis according to a “–AB–AB–” sequence. Inside each plane, Mn atoms form a kagome-type lattice with Ga, Ge, or Sn lying

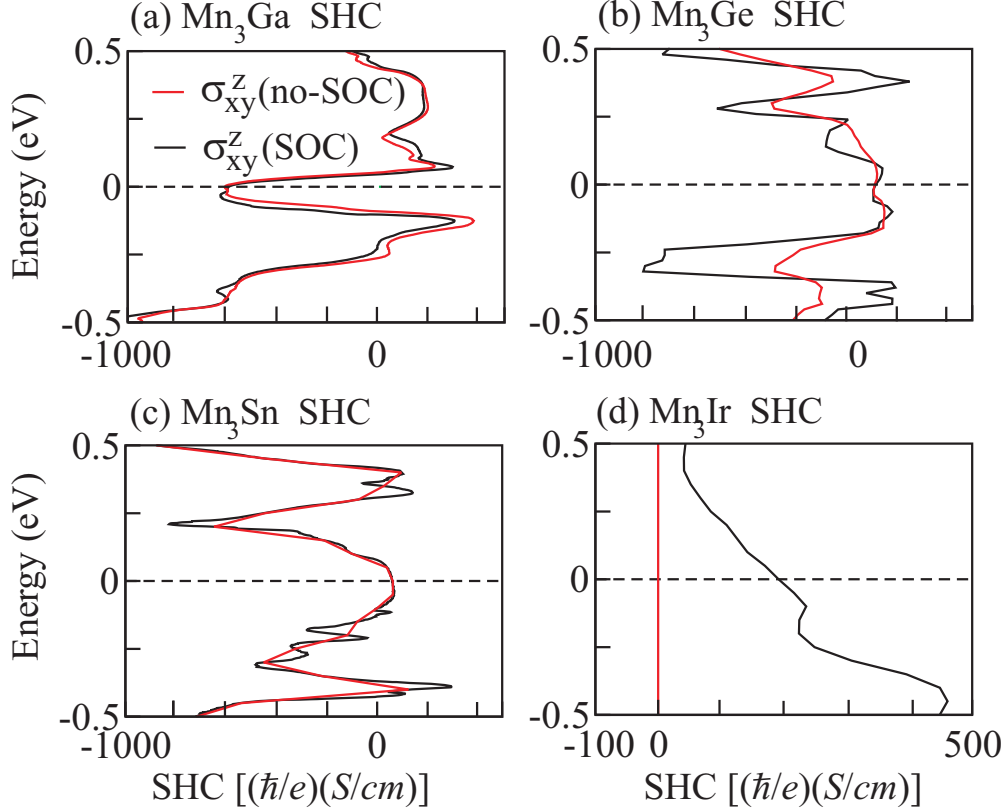


FIG. 4. Energy-dependent SHC tensor elements of σ_{xy}^z with and without SOC for (a) Mn_3Ga , (b) Mn_3Ge , (c) Mn_3Sn , and (d) Mn_3Ir . The Fermi energy is indicated by the dashed horizontal line.

at the center of the hexagon formed by Mn. Both the *ab initio* calculation³¹ and neutron diffraction measurements^{35–37} show that the Mn magnetic moments exhibit noncollinear AFM order, where the neighboring moments are aligned at an angle of 120° , as in Fig. 2(b). Large AHE in room temperature has recently been reported in Mn_3Ge and Mn_3Sn .^{22,23} These materials also exhibit other exotic phenomena including the Weyl semimetal phase,³⁸ magneto-optical Kerr effect,³⁹ anomalous Nernst effect,⁴⁰ and topological defects.⁴¹ Distinct from hexagonal Mn_3X compounds, the Mn_3Ir (space group $Pm\bar{3}m$, No. 221) crystallizes in a face-centered cubic structure with Mn atoms in the $[111]$ planes forming a kagome lattice with the $q = 0$ magnetic order.

The symmetry of the SHE without SOC in these materials can be understood using a similar approach as we used for the 2D kagome lattice. The hexagonal Ga, Ge, and Sn materials can be viewed as stacking versions of the kagome lattice and thus we find that the symmetry of SHE is the same as the 2D kagome lattice, i.e. only $\sigma_{xy}^z = -\sigma_{yx}^z$ is nonzero.

However, we find that SHE must vanish in Mn_3Ir without SOC, which is imposed by the higher symmetry of the cubic magnetic lattice. For completeness, we list the tensor matrices without and with SOC for all these compounds in the appendix.

Since the SHC tensor shape imposed by the symmetry has been systematically investigated for these materials in Ref. 34, we only discuss one of the largest SHC tensor elements σ_{xy}^z based on the *ab initio* calculations⁴² of the SHC. For comparison, we show the SHC without and together with SOC in Fig. 4. In the absence of SOC, Ga, Ge, and Sn compounds indeed exhibit nonzero SHC $\sigma_{xy}^z = -613, 115, \text{ and } 90 (\hbar/e)(\Omega \cdot \text{cm})^{-1}$, respectively, at the Fermi energy. One can see that SOC induces very few changes in the band structure and thereafter modifies the SHC weakly, especially at the Fermi energy for Ga, Ge, and Sn compounds. It is intuitive to observe comparable σ_{xy}^z values for Ge and Sn compounds, despite the fact that Sn exhibits much larger SOC than Ge. These facts further verifies that the noncollinear magnetic structure, rather than SOC, is dominant for the SHE. The Ga compound shows an opposite sign in SHC compared to the Ge/Sn compound, since Ga has one valence electron fewer than Ge/Sn and the Fermi energy is lower in Mn_3Ga than in $\text{Mn}_3\text{Ge}/\text{Mn}_3\text{Sn}$.

III. DISCUSSION

Understanding the role SOC plays in the SHE is important for the fundamental understanding of the SHE, but also for practical reasons. It can help with the search for materials with large SHE since in non-magnetic or collinear magnetic materials, SOC is necessary for SHE and thus the presence of heavy elements is generally required for large SHE. The SHE without SOC proposed in this work suggests a new strategy to design SHE materials without necessarily involving heavy elements. In noncollinear systems, the Rashba effect can also appear without SOC⁴³. The spin texture in the band structure may depend sensitively on the real space spin texture. For example, we found that band structure spin texture is different between the Kagome lattice and the triangular lattice.

We propose the general, necessary symmetry-breaking requirements (Fig. 1) for SHE without SOC. It is worth noting that SHE can become zero without SOC in some non-collinear magnetic lattice where additional symmetries forces the SHE to vanish. For example, we have shown that in Mn_3Ir the SHE vanishes in absence of SOC even though it

has a noncollinear magnetic structure. This is a consequence of its high-symmetrical cubic structure. Similar situation could happen for AHE without SOC in a noncoplanar magnetic lattice, such as the AFM skyrmion system²¹.

In conclusion, we have shown that the SHE can be realized by a non-chiral coplanar magnetic structure without involving the SOC. The noncollinearity of the magnetic lattice can break the spin rotation symmetry and consequently allow the existence of SHE. By *ab initio* calculations, we further predicted that such an SHE without SOC can be observed in noncollinear AFM compounds Mn_3X ($X = Ga, Ge, \text{ and } Sn$). From our symmetry considerations, an extrinsic SHE can appear when breaking the spin rotational symmetry. Thus, we expect the extrinsic effect to also exist in our systems. Its amplitude will depend on the details of the scattering, and cannot be estimated without microscopic calculations, though in general for SHE the intrinsic contribution tends to be the dominant contribution. By providing a general theoretical, symmetry based understanding of the SHE, our work motivates a comprehensive search for SHE materials among noncollinear magnetic systems, that not necessarily involve heavy elements. In addition, the close relation between the SHE and the magnetic order suggests that the SHE may be used vice versa, as a probe to establish and symmetry restrict the ground state magnetic structures of long-range ordered antiferromagnets.

Regarding the strong correlated system, we would discuss the spin liquid material as an example. $RuCl_3$ has a rich magnetic phase diagram, with a complex zig-zag type AFM long-range order at low temperatures, and even a quantum spin liquid phase in applied magnetic field. According to our work, non-magnetic and collinearly ordered phases have vanishing SHE without SOC. For the quantum spin liquid phase, it remains unclear whether SHE appears without SOC. If yes, SHE would be a promising probe to the spin liquid phase. We will study this very interesting question in the future.

IV. METHOD

To calculate the SHE in these compounds we obtain the DFT Bloch wave functions from Vienna *ab-initio* Simulation Package (VASP)⁴² within the generalized gradient approximation (GGA).⁴⁴ By projecting the Bloch wave functions onto maximally localized Wannier functions (MLWFs),⁴⁵ we get a tight-binding Hamiltonian which we use for efficient evalua-

tion of the SHC. For the integrals of Eq. 3, the BZ was sampled by k -grids from $50 \times 50 \times 50$ to $200 \times 200 \times 200$. Satisfactory convergence was achieved for a k -grid of size $150 \times 150 \times 150$ for all three compounds. Increasing the grid size to $200 \times 200 \times 200$ only varied the SHC by no more than 5%. The results of the calculations agree well with the symmetry analysis.

V. ACKNOWLEDGMENTS

We thank Prof. Claudia Felser at Max Planck Institute in Dresden and Prof. Carsten Timm at the Technical University Dresden, Prof. Yuval Oreg in the Weizmann Institute of Science for helpful discussions. Y.Z. and J.v.d.B. acknowledge the German Research Foundation (DFG) SFB 1143. Y.Z. and J.Z. acknowledge the the ASPIN project (EU FET Open RIA Grant No. 766566 grant (ASPIN)). B.Y. acknowledges the support by the Ruth and Herman Albert Scholars Program for New Scientists in Weizmann Institute of Science and by a Grant from the GIF, the German-Israeli Foundation for Scientific Research and Development.

VI. AUTHOR CONTRIBUTIONS

B.Y. conceived the project. Y.Z., J.Z. and Y.S. performed the DFT calculation and the data analysis. Y.Z., J.Z., and B.Y. performed the tight-binding modeling and symmetry analysis. Y.Z. wrote the manuscript with contributions from all co-authors. J.v.d.B. and B.Y. supervised the work. We acknowledge the support by ASPIN (EU FET Open RIA Grant No. 766566).

VII. COMPETING INTERESTS

The authors declare no competing financial interests.

* binghai.yan@weizmann.ac.il

¹ J. Sinova, S. O. Valenzuela, J. Wunderlich, C. Back, and T. Jungwirth, Reviews of Modern Physics **87** (2015).

- ² S. A. Wolf, D. D. Awschalom, R. A. Buhrman, J. M. Daughton, S. von Molnár, M. L. Roukes, A. Y. Chtchelkanova, and D. M. Treger, *Science* **294**, 1488 (2001).
- ³ S. Maekawa, S. O. Valenzuela, E. Saitoh, and T. Kimura, *Spin Current*, Vol. 17 (Oxford University Press, 2012).
- ⁴ A. Hoffmann, *IEEE Trans. Magn.* **49**, 5172 (2013).
- ⁵ M. Gradhand, D. Fedorov, F. Pientka, P. Zahn, I. Mertig, and B. L. Györffy, *Journal of Physics: Condensed Matter* **24**, 213202 (2012).
- ⁶ I. M. Miron, K. Garello, G. Gaudin, P.-J. Zermatten, M. V. Costache, S. Auffret, S. Bandiera, B. Rodmacq, A. Schuhl, and P. Gambardella, *Nature* **476**, 189 (2011).
- ⁷ L. Liu, C.-F. Pai, Y. Li, H. W. Tseng, D. C. Ralph, and R. A. Buhrman, *Science* **336**, 555 (2012).
- ⁸ S. Parkin and S.-H. Yang, *Nature Nanotech* **10**, 195 (2015).
- ⁹ S.-H. Yang, K.-S. Ryu, and S. Parkin, *Nature Nanotech* **10**, 221 (2015).
- ¹⁰ N. Nagaosa, J. Sinova, S. Onoda, A. H. MacDonald, and N. P. Ong, *Reviews of Modern Physics* **82**, 1539 (2010).
- ¹¹ S. Murakami, N. Nagaosa, and S.-C. Zhang, *Science* **301**, 1348 (2003).
- ¹² J. Sinova, D. Culcer, Q. Niu, N. A. Sinitsyn, T. Jungwirth, and A. H. MacDonald, *Phys. Rev. Lett.* **92**, 126603 (2004).
- ¹³ D. Xiao, M.-C. Chang, and Q. Niu, *Rev. Mod. Phys.* **82**, 1959 (2010).
- ¹⁴ K. Ohgushi, S. Murakami, and N. Nagaosa, *Physical Review B* **62**, R6065 (2000).
- ¹⁵ Y. Taguchi, Y. Oohara, H. Yoshizawa, N. Nagaosa, and Y. Tokura, *Science* **291**, 2573 (2001).
- ¹⁶ P. Bruno, V. K. Dugaev, and M. Taillefumier, *Phys. Rev. Lett.* **93**, 096806 (2004).
- ¹⁷ A. Neubauer, C. Pfleiderer, B. Binz, A. Rosch, R. Ritz, P. G. Niklowitz, and P. Böni, *Phys. Rev. Lett.* **102**, 186602 (2009).
- ¹⁸ N. Kanazawa, Y. Onose, T. Arima, D. Okuyama, K. Ohoyama, S. Wakimoto, K. Kakurai, S. Ishiwata, and Y. Tokura, *Phys. Rev. Lett.* **106**, 156603 (2011).
- ¹⁹ G. Yin, Y. Liu, Y. Barlas, J. Zang, and R. K. Lake, *Phys. Rev. B* **92**, 024411 (2015).
- ²⁰ P. M. Buhl, F. Freimuth, S. Blügel, and Y. Mokrousov, *arXiv:1701.03030* (2017).
- ²¹ P. B. Ndiaye, C. A. Akosa, and A. Manchon, *Physical Review B* **95**, 064426 (2017).
- ²² A. K. Nayak, J. E. Fischer, Y. Sun, B. Yan, J. Karel, A. C. Komarek, C. Shekhar, N. Kumar, W. Schnelle, J. Kuebler, C. Felser, and S. S. P. Parkin, *Science Advances* **2**, 150187 (2016).

- ²³ S. Nakatsuji, N. Kiyohara, and T. Higo, *Nature* **527**, 212 (2015).
- ²⁴ C. Zener, *Phys. Rev.* **82**, 403 (1951).
- ²⁵ P. W. Anderson and H. Hasegawa, *Phys. Rev.* **100**, 675 (1955).
- ²⁶ P. G. de Gennes, *Phys. Rev.* **118**, 141 (1960).
- ²⁷ D. B. Litvin and W. Opechowski, *Physica* **76**, 538 (1974).
- ²⁸ W. F. Brinkman and R. J. Elliott, *Proc. R. Soc. London, Ser. A* **294**, 343 (1966).
- ²⁹ M. Seemann, D. Koedderitzsch, S. Wimmer, and H. Ebert, *Phys. Rev. B* **92**, 155138 (2015).
- ³⁰ H. Chen, Q. Niu, and A. MacDonald, *Phys. Rev. Lett.* **112**, 017205 (2014).
- ³¹ D. Zhang, B. Yan, S.-C. Wu, J. Kübler, G. Kreiner, S. S. Parkin, and C. Felser, *Journal of Physics: Condensed Matter* **25**, 206006 (2013).
- ³² J. Kübler and C. Felser, *EPL* **108**, 67001 (2014).
- ³³ W. Zhang, W. Han, S. H. Yang, Y. Sun, Y. Zhang, B. Yan, and S. Parkin, *Science Advances* **2**, e1600759 (2016).
- ³⁴ Y. Zhang, Y. Sun, H. Yang, J. Železný, S. P. P. Parkin, C. Felser, and B. Yan, *Phys. Rev. B* **95**, 075128 (2017).
- ³⁵ E. Krén and G. Kádár, *Solid State Communications* **8**, 1653 (1970).
- ³⁶ G. Kádár and E. Krén, *International Journal of Magnetism* **1**, 43 (1971).
- ³⁷ T. Ohoyama, K. Yasuköchi, and K. Kanematsu, *Phys. Soc. Japan* **16**, 325 (1961).
- ³⁸ H. Yang, Y. Sun, Y. Zhang, W.-J. Shi, S. S. P. Parkin, and B. Yan, *arXiv:1608.03404* (2016).
- ³⁹ W. Feng, G.-Y. Guo, J. Zhou, Y. Yao, and Q. Niu, *Phys. Rev. B* **92**, 144426 (2015).
- ⁴⁰ X. Li, L. Xu, L. Ding, J. Wang, M. Shen, X. Lu, Z. Zhu, and K. Behnia, *arXiv:1612.06128* (2016).
- ⁴¹ J. Liu and L. Balents, *arXiv:1703.08910* (2017).
- ⁴² G. Kresse and J. Furthmüller, *Phys. Rev. B* **54**, 11169 (1996).
- ⁴³ Q. Liu, Y. Guo, and A. J. Freeman, *Nano letters* **13**, 5264 (2013).
- ⁴⁴ J. P. Perdew, K. Burke, and M. Ernzerhof, *Phys. Rev. Lett.* **77**, 3865 (1996).
- ⁴⁵ A. A. Mostofi, J. R. Yates, Y.-S. Lee, I. Souza, D. Vanderbilt, and N. Marzari, *Comput. Phys. Commun.* **178**, 685 (2008).